# CORE-MONITORING IN CANDU REACTORS USING IN-CORE DETECTORS

B. Arsenault
Atomic Energy of Canada Limited
2251 Speakman Drive
Mississauga, Ontario
Canada
L5K 1B2
arsenaultb@aecl.ca

## ABSTRACT

CANada Deuterium Uranium (CANDU®) reactors are provided with in-core detectors, that are used for regulation, protection, and flux mapping. A set of 28 in-core platinum detectors is used in the reactor regulating system (RRS). The RRS maintains a target core power distribution by manipulating the individual amounts of light water in zone-control compartments, one for each of 14 defined control zones.

In-core platinum detectors are also used in reactor protection systems. One such protection system is dedicated to each of the two independent CANDU emergency shutdown systems, SDS-1 and SDS-2. These detectors constitute what is called the regional overpower protection (ROP) system. In the ROP system for each special shutdown system, the detectors are grouped into three safety logic channels, and triplicated logic is used to actuate the associated shutdown system.

CANDU reactors also use a system of self-powered detectors for flux mapping. The electrical signal generated by the detectors is amplified, and corrections are made for individual detector sensitivity, based on detector irradiation. The signals from these vanadium flux-mapping detectors have been used to validate the reactor-core physics calculations, by comparing the calculated and measured fluxes at the detector locations. Very good agreement is typically obtained between calculated and measured fluxes for the period of reactor history reported in this paper the standard deviation was $2.64\% \pm 0.08\%$.

---

®CANDU is a registered trademark of Atomic Energy of Canada Limited (AECL)

# 1. INTRODUCTION

CANDU reactors are pressure-tube reactors.  Each pressure tube is surrounded by a concentric calandria tube, which insulates it from the surrounding heavy-water moderator.  The reactor is refuelled with natural-uranium fuel.  Reactivity mechanisms are located vertically and horizontally across the calandria, interstitially between the calandria tubes.

The main reactivity mechanisms used by the reactor regulating system (RRS) to control the power distribution are liquid zone controllers and adjuster rods.  The RRS uses an in-core monitoring system.  The liquid zone controller system consists of 14 light-water compartments oriented vertically in the core.  Figure 1 shows the light-water compartments with the reactor zone-control-detector assemblies.  The core flux distribution is controlled by the amount of light water in the various liquid zone compartments.  The RRS also uses adjuster rods, which are vertical mechanisms made of stainless-steel or cobalt.  They serve 2 purposes: they provide axial and radial flattening to improve the power shape, and they provide on removal a reactivity-shim or xenon-override capability.  These 2 reactivity systems are controlled by the RRS by means of an in-core monitoring system, to control the reactor power within an operating envelope.

CANDU reactors have two independent shutdown systems that can be actuated by the in-core reactor protection system and that are able to effect a rapid reactor shutdown.  Shutdown system number one (SDS-1) consists of cadmium absorbers inserted vertically into the reactor from top to bottom. Shutdown system number two (SDS-2) injects a neutron absorbing liquid (gadolinium nitrate solution) directly into the moderator via horizontal nozzles that traverse the reactor core.

# 2. TYPES OF SELF-POWERED NEUTRON DETECTORS USED IN CANDU REACTORS

There different in-core detector systems are used in CANDU reactors for regulation, protection, and flux mapping respectively.  Table I lists the neutron-flux instrumentation systems used in CANDU reactors, along with their associated applications.

The RRS uses different detector types, each designed for a given operating range with an overlap of 1 decade between the neutron instrumentation types.  Proportional counters are used for startup flux measurements.  They are made of tubes filled with $BF_3$, enriched in $^{10}B$.  $BF_3$ counters are for temporary use in subcriticality monitoring during the approach to criticality.  After following reactor commissioning they are removed from the core.

The ion chambers consist of two concentric cylinders coated with $^{10}B$.  Thermal neutron capture by $^{10}B$ releases alpha particles, which ionize hydrogen gas.  An applied DC high voltage collects the resulting electrons from the ionized hydrogen gas.  The signal generated by the ion chambers is fully prompt and covers a range from $10^6$ to 1.5 full power (FP).  Ion chambers are used for 2 purposes: flux regulation at low power, and power measurements for SDS-1 and SDS-2.

The in-core flux detectors are self-powered in-core flux detectors. The design consists of an emitter wire and an outer sheath or collector, which are separated by MgO insulation. The detector is approximately 3 mm in outer diameter, with a similar co-axial 1-mm cable. Three types of reactions can occur in the self-powered in-core flux detectors: $(n,\beta)$, $(n,\gamma,e)$, and $(\gamma,e)$. The reactions cause a net flow of electrons proportional to the incident neutron flux to flow from the central emitter to the sheath. Four types of self-powered detectors can be used, with vanadium emitter material as follows:

- Vanadium: The dominant reaction is $(n,\beta)$, and the response is approximately 92% delayed. Vanadium detectors are used for flux mapping.
- Platinum: The response is 85% prompt and a dynamic compensation is required if they are to be used in a safety system.
- Pt-clad Inconel: The response is 91% prompt, and the burnup characteristics are complex. These detectors are used in the reactor-protection system (which actuates SDS-1 or SDS-2) and in the RRS.
- Solid Inconel: The response is 102% prompt.

In the normal operating power range, self-powered detectors are used because the ion chambers located outside the core do not provide the accuracy required for spatial control. The range of sensitivity for each of the detector types is given in Figure 2.

The vanadium detectors are more sensitive to thermal neutrons, but the time response depends on the beta decay of vanadium-52 (3.76-min half-life).

Half of the response of the platinum detector types comes from the thermal-neutron response. The other half comes from the response to gamma rays. Platinum detectors respond promptly, but since one third of the gamma radiation is delayed, the detector response is approximately 85% prompt. The response of fuel power to a step increase in neutron flux is ~95% prompt. The detector signals use dynamic compensation in safety applications to take into account the 10% difference.

The signals generated by the vanadium detectors needs to be corrected as a function of the burnup. A correction is applied as a function of the integrated detector signal based on predicted detector burnups.

## 2.1 DETECTOR DESIGNS

The vanadium and platinum detectors, also called straight individually replaceable (SIR) detectors, are made of an emitter surrounded by an insulator contained in a collector. Figure 3 shows vanadium and platinum-clad Inconel detectors. The SIR concept was introduced to allow the replacement of defective detectors at a minimum cost and a reduced man-rem burden (Reference 1). The concept consists of detector guide tubes enclosed in a dry assembly with a shield plug to block streaming radiation. The connector housing can be opened to allow a replacement detector to be inserted into a spare well. One or more detectors can be withdrawn

without the need to remove the entire flux detector unit. One well tube is also reserved at the centre of the well for a travelling flux detector (TFD). A TFD is a miniature fission chamber that can be inserted the full length of the assembly to scan and measure the thermal neutron-flux distribution. The TFD can be used to confirm the response of detectors in the assembly.

## 3. THE REACTOR REGULATING SYSTEM

The RRS has two main functions, bulk control of the core reactivity and spatial control of the flux distribution. To achieve these functions, the RRS uses the in-core platinum-clad Inconel detectors. Two detectors are used in each of the 14 zones of the reactor. The signals generated by these detectors are fed to the RRS, which automatically controls the amount of light water contained in each liquid zone compartment. The 14 light-water compartments are manipulated uniformly for bulk control and differentially to achieve the desired spatial flux distribution.

Additionally, the RRS can also control the insertion and withdrawal of adjusters and mechanical control absorbers (MCAs) to extend the reactivity range provided by the liquid zone controllers. The MCAs are driven in when the average liquid zone fill is greater than 80% or if there is a large positive power error. The MCAs are driven out when the average liquid zone fill is less than 70% or if the power error is negative.

## 4. REGIONAL OVERPOWER PROTECTION SYSTEM

A safety system, called the regional overpower protection (ROP) system, has been designed for CANDU reactors. The ROP system ensures that in the event of a slow loss-of-regulation (LOR) accident, the reactor is tripped before a dryout occurs in any of the fuel channels. The ROP system consists of two independent arrays of detectors one set for each shutdown system. These monitor neutron flux and are arrayed through the core. Figure 4 shows the location of some of the detectors used for SDS-2.

Regional overpower protection setpoints are set so that the neutron flux exceeds the setpoint, in some ROP detectors, before the channel power exceeds the critical channel power in any fuel channel. The critical channel powers are defined as the onset of intermittent dryout in a fuel channel.

The detectors are subdivided into three logic channels for each of the 2 safety systems; D, E and F for SDS-1 and G, H and J for SDS-2. If the reading of any one detector in a logic channel reaches its setpoint, that channel is tripped. When 2 logic channels are tripped, the corresponding shutdown system is actuated. Figure 5 shows the triplicated logic used for SDS-1. A sufficient nnumber of detectors must exceed the ROP setpoint to actuate a shutdown system. This applies to any slow LOR accident scenario initiated from normal operation.

For each postulated slow LOR accident scenario, the Reactor Fuelling Simulation Program - Industry Standard Tool Set (RFSP-IST) is used to calculate the neutron flux and time-average

thermal powers in the core (Reference 2). The time-average power is calculated for each fuel bundle and channel. The neutron flux is calculated for each ROP detector. Ripples are defined as the deviation of instantaneous channel powers from the nominal time-average channel powers. Combining the ripples with the time-average powers for each of the postulated accident scenarios, the resulting channel powers can be determined as a combination of many accident scenarios and instantaneous snapshots in the reactor operating history.

## 5. FLUX MAPPING AND VALIDATION OF REACTOR PHYSICS CALCULATIONS USING IN-CORE VANADIUM DETECTORS

The CANDU design is provided with a flux-mapping system to synthesize the 3-dimensional flux distribution in the reactor from in-core detector readings. The system consists of 102 vanadium detectors placed at various positions in the core. Each detector is one lattice pitch long.

The flux-mapping procedure consists of assuming the 3-dimensional flux distribution can be written as a linear combination of a number of basis functions or flux modes, i.e. that the thermal flux at any point $r$ in the core, $\phi(r)$, can be expressed as a linear combination of flux modes $\psi_n(r)$:

$$f(r) = \sum_{n=1}^{m} A_n y_n(r) \tag{5.1}$$

where m is the total number of modes used, and $A_n$ is the amplitude of the $n^{th}$ mode.

Using this linear expansion, the mode amplitudes $A_n$ are determined by a least-squares fit of the calculated fluxes at the 102 detectors to the measured fluxes. For a detector d at position $r_d$, the mapped flux is, from Equation 5.1:

$$f(r_d) = \sum_{n=1}^{m} A_n y_n(r_d) \tag{5.2}$$

and this can be compared to the measured flux at the detector, $F_d$.

The flux-mapping procedure determines the amplitudes $A_n$ by minimizing the sum $\varepsilon$ of squares of differences between the mapped and measured fluxes, i.e. minimizing

$$e = \sum_{d=1}^{102} w_d (f_d - F_d)^2 \tag{5.3}$$

where the $w_d$ are chosen weights.

Once the amplitudes have been evaluated, the flux at any point in the reactor can be calculated very easily from Equation 5.1. Thus the 3-dimensional flux and power distributions in the core can be derived. The flux-mapping procedure is very quick.

The flux modes $\psi_n(r)$ used in flux mapping consist in the first instance of a number (~15) of pre-calculated harmonics of the neutron diffusion equation. These harmonics represent various possible global perturbations of the flux distribution.

For situations in which the reactor is operated with mechanical control absorbers in-core or adjusters out-of-core, the harmonics are complemented by a number of "device modes" that represent the more localized perturbations that are due to device movement.

The flux-mapping procedure is conducted automatically in the on-line computer every 2 min. It provides the mapped values of average zonal flux to the regulating system. These zonal fluxes are used to calibrate the zone-control detectors, to ensure that the readings of the zone detectors faithfully represent the overall flux distribution in the reactor.

Flux mapping can also be done "off line", using recorded flux measurements at the detectors corresponding to any desired time in the reactor history. The measurements are compared with the simulated values, and the results are analyzed by grouping sections of the reactor core model to highlight weaknesses of the calculation tools.

## 5.1 INTERPOLATION IN THE THERMAL NEUTRON-FLUX DISTRIBUTION OF THE VANADIUM DETECTORS

It is necessary to calculate the thermal neutron flux at points other than those where the solution of the finite-difference diffusion equation provides flux values. This occurs for instance when flux at in-core detectors (flux-mapping or protection system) is required. This section describes the procedure within the code to interpolate in the macroscopic flux distribution calculated by the RFSP-IST code. It should be noted that this interpolation is not equivalent to reconstructing the microscopic flux within the cell from a knowledge of the results of a cell code.

The function of interpolation in the thermal-flux distribution is performed by the *INTREP module of the RFSP-IST code. With this module it is possible to define the positions of detectors. Detectors are defined into groups and are specified as vertical or horizontal detectors. Since detectors typically occupy a non-negligible length along an assembly, the user has the option of subdividing each detector into a number of segments for purposes of calculating the average flux seen by the detector.

Parabolic interpolation in the x, y, and z directions is used to compute the thermal flux at the centre of each detector segment from the three-dimensional thermal-flux distribution. The average flux at a detector is then obtained by averaging these segment fluxes.

## 5.2 REACTOR-CORE SIMULATIONS

CANDU reactor-core simulations are done with the RFSP-IST code. An important type of simulation performed with RFSP-IST is referred to as local-parameter calculations. In history-based simulations, local parameters describing the values of physical parameters (fuel temperature, coolant temperature, coolant density, coolant purity, moderator poison, moderator temperature and moderator purity) at each bundle location are used in the calculation of the lattice-cell properties. The lattice-cell properties are then used in RFSP-IST, to calculate a new approximation to the neutron flux distribution, and lattice-cell and core-flux calculations are performed iteratively until a self-consistent solution is obtained. Current requirements for code validation, as well as the need to analyze new fuel and reactor designs, have led to the choice of the more theoretically rigorous WIMS-AECL code (Reference 3) as the lattice-cell calculation for CANDU analyses in the future.

The application of a lattice-cell code such as WIMS-AECL poses some challenges to reactor core analyses, especially in the area of history-based analyses. In principle, WIMS-AECL could be used in conventional calculations to generate the local parameters of all the bundles to be used in history-based CANDU core calculations. However, each lattice-cell calculation with WIMS-AECL requires approximately 5 s of computation on typical workstations. Therefore, the conventional approach would be unsuitable for a typical RFSP-IST history-based calculation that requires an average of 30,000 lattice-cell calculations because the roughly 40 h of computation per core burnup step is impractical.

To overcome the computation-time problem implicit in the use of a lattice-cell code such as WIMS-AECL, a simple-cell lattice-cell calculation methodology has been developed. At the specific states used to determine the parameters defining the simple-cell model, the simple-cell approach accurately reproduces WIMS-AECL results important for reactor simulations and requires a computation time of the order of 200 times less than standard WIMS-AECL lattice-cell calculations. Interfacing the simple-cell model with RFSP-IST makes history-based calculations consistent with WIMS-AECL results.

## 5.3 DESCRIPTION OF THE SIMPLE-CELL MODEL

The simple-cell model calculates the neutron-flux distributions within a lattice cell with homogenized-region one-dimensional multigroup diffusion theory, rather than two-dimensional multigroup transport theory that is applied in WIMS-AECL. Using the superhomogenization (SPH) procedure (Reference 4), the homogenized-region cross sections to be used in this calculation can be formed in such a manner that the cell-average neutron fluxes, region-averaged reactions and eigenvalues of reference WIMS-AECL solutions are preserved for the specific fuel types for which the models were prepared. These homogenized-region cross sections are stored in "simple-cell fuel tables" and are transferred to RFSP-IST. Reference 5 gives additional information on the simple-cell model.

## 5.4 DESCRIPTION OF THE REACTOR CORE SIMULATIONS

A 1-a core follow of a CANDU reactor was simulated with RFSP-IST from full power day (FPD) 3861.5 through FPD 4214.9. The reactor core modelled in RFSP-IST was a full CANDU reactor with the fuel bundles represented by homogenized lattice cell regions. The properties of the lattice cells were calculated with the simple-cell model where the fuel, heavy-water coolant, the pressure tube, calandria tube, and the heavy-water moderator were homogenized in one region. The lattice properties for each fuel bundle were calculated with the local-parameter approach to have a better accuracy in the isotopic concentrations. The heavy-water reflector surrounding the fuel channels and the notches at each end of the reactor were also modelled in RFSP-IST. The incremental cross sections of the structural materials such as the springs, locators, brackets, etc were included as well. The incremental cross sections of the reactivity devices and guide tubes were also modelled.

Four global parameters were specified in each of the reactor-core input files to reflect the measured values obtained during the simulated period. The 4 global parameters were: the moderator temperature, moderator purity, moderator boron, and the coolant purity. Coolant temperatures and coolant densities at each bundle location were calculated by a thermalhydraulic code (NUCIRC) and were used by RFSP-IST. The individual levels of the liquid zone compartments used in the simulations were based on the measured levels obtained during the operating period.

The neutron flux values calculated with RFSP-IST at each simulation step were used to interpolate the thermal neutron flux values at each vanadium detector site. The interpolated thermal neutron flux values were compared with the measured detector readings. The results of the comparisons are given in terms of the standard deviation of percent differences between calculated and measured detector fluxes.

## 6. RESULTS OF THE SIMULATIONS

The results of the simulations obtained with the simple-cell history-based method are shown in Figure 6. The figure shows a constant decrease in the standard deviation from the start of the simulations up to ~4000 FPDs. The constant decrease comes from a stabilization period required in the simulations when switching to the new simple-cell approach. Therefore, the average and root-mean-square (RMS) values were based on the subset of data in the range between FPD 4000 and FPD 4214.9. The percent difference was 2.64% with an RMS value of 0.08%.

The figure also shows that the standard deviation increased significantly on 3 occasions. The first one was at FPD 3874.5, which corresponds approximately to 5 FPDs after the first shutdown. The simulations were done at 100% full power without taking into account the shutdown period. Therefore, the difference in the standard deviation at FPD 3874.5 was explained by a discrepancy in the calculated and actual isotopic concentrations. The second and third increases occurred at FPD 3956.8 and FPD 4131.8. These 2 peaks occurred because the vanadium detector signals for these 2 cases were taken at a reduced power of about 77% to 80% full power whereas the

simulations were done at full power.  The xenon load in the simulations calculated at a 100% full power differed from the xenon load during the vanadium readings (80% FP), leading to a different flux shape, and thereby, increasing the standard deviation.  The average value was calculated with the results of the simulations obtained from FPD 4000 to FPD 4214.9.  The peak obtained at FPD 4131.8 was not included in the calculation of the average value.

## 7. CONCLUSIONS

Core monitoring by means of in-core detectors is used extensively in CANDU reactors. Detectors of various types are used in various applications, regulation and, protection systems and in flux mapping.

CANDU 3-dimensional flux mapping is validated by a comparison of the simulated neutron-flux values with the measured in-core vanadium readings.  The excellent agreement (percent difference of 2.64% with an RMS of 0.08%) for the period reported here is typical of the results obtained.

**REFERENCES**

1.  J.M. Cutler and N. Medak, "New Flux Detectors for CANDU 6 Reactors", In Proceedings of the 1992 CAN/CNS Joint Annual Conference, Saint-John, Canada, 1992 June.
2.  D.A. Jenkins, B. Arsenault, A.U. Rehman and W.M. Kelly, "Update on RFSP-IST", In Proceedings of the 21$^{st}$ Annual Conference of the Canadian Nuclear Society, Toronto, Canada, 2000 June.
3.  J. Griffiths, "WIMS-AECL User's Manual", Atomic Energy of Canada Limited Report, RC-1176, 1994 March.
4.  A. Hebert and G. Mathionniere, "Development of a Third-Generation Superhomogenization Method for the Homogenization of a Pressurized Water Assembly", Nuclear Science and Engineering, **115**, 124-141, 1993.
5.  J.V. Donnelly, "Development of a Simple-Cell Model for Performing History-Based RFSP Simulations with WIMS-AECL", In Proceedings of the 1998 International Conference on the Physics of Nuclear Science and Technology, Long Island, New York, 1998 October.

Table I: Neutron-Flux Instrumentation

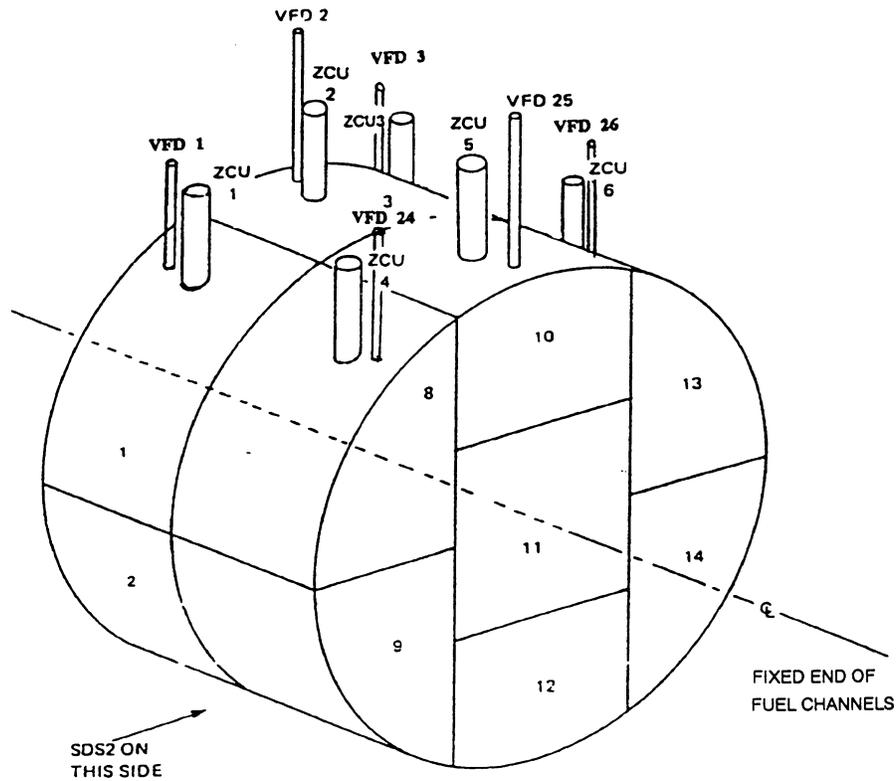| Detector Type | Flux Mapping | Flux Regulation | SDS-1 | SDS-2 |
|---|---|---|---|---|
| Proportional Counters (BF$_3$) | | 3 In-Core Counters for $10^{-14}$ to $10^{-9}$ FP, 3 Out-of-Core Detectors for $10^{-10}$ to $10^{-6}$ FP | | |
| Ion Chambers | | 3 Out-of-Core Detectors for $10^{-6}$ to 0.15 FP | 3 Out-of-Core Detectors | 3 Out-of-Core Detectors |
| Flux Detectors | 102 In-Core Vanadium Detectors | 28 In-Core Platinum Detectors | 34 In-Core Platinum Detectors | 24 In-Core Platinum Detectors |



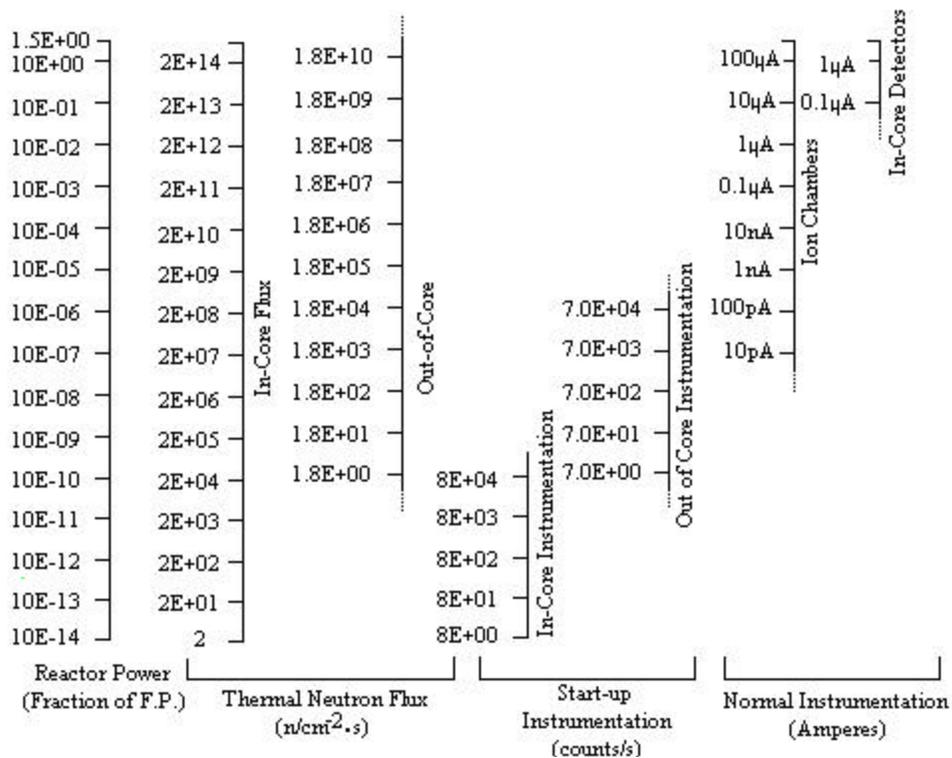Figure 1: Light-Water Compartments and the Reactor Zone Control Detector Assemblies

Figure 2 chart:

Reactor Power (Fraction of F.P.):
1.5E+00
10E+00
10E-01
10E-02
10E-03
10E-04
10E-05
10E-06
10E-07
10E-08
10E-09
10E-10
10E-11
10E-12
10E-13
10E-14

Thermal Neutron Flux ($n/cm^2 \cdot s$) — In-Core Flux:
2E+14
2E+13
2E+12
2E+11
2E+10
2E+09
2E+08
2E+07
2E+06
2E+05
2E+04
2E+03
2E+02
2E+01
2

Out-of-Core:
1.8E+10
1.8E+09
1.8E+08
1.8E+07
1.8E+06
1.8E+05
1.8E+04
1.8E+03
1.8E+02
1.8E+01
1.8E+00

Start-up Instrumentation (counts/s) — In-Core Instrumentation:
8E+04
8E+03
8E+02
8E+01
8E+00

Out of Core Instrumentation:
7.0E+04
7.0E+03
7.0E+02
7.0E+01
7.0E+00

Normal Instrumentation (Amperes) — Ion Chambers:
100µA
10µA
1µA
0.1µA
10nA
1nA
100pA
10pA

In-Core Detectors:
1µA
0.1µA

Figure 2: Range of Sensitivity of Nuclear Instrumentation

VANADIUM
3.0 mm OD
~ 1.7 mm OD EMITTER
INCONEL 600
MgO

PLATINUM-CLAD INCONEL
3.0 mm OD
~ 1.7 mm OD EMITTER
INCONEL 600
LAYER OF PLATINUM (~0.1 mm THICK)
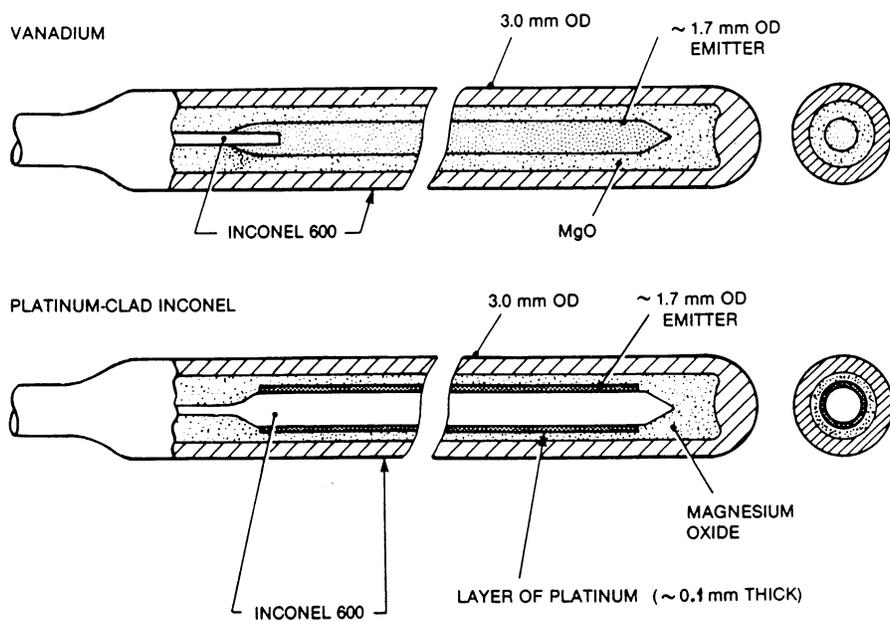MAGNESIUM OXIDE
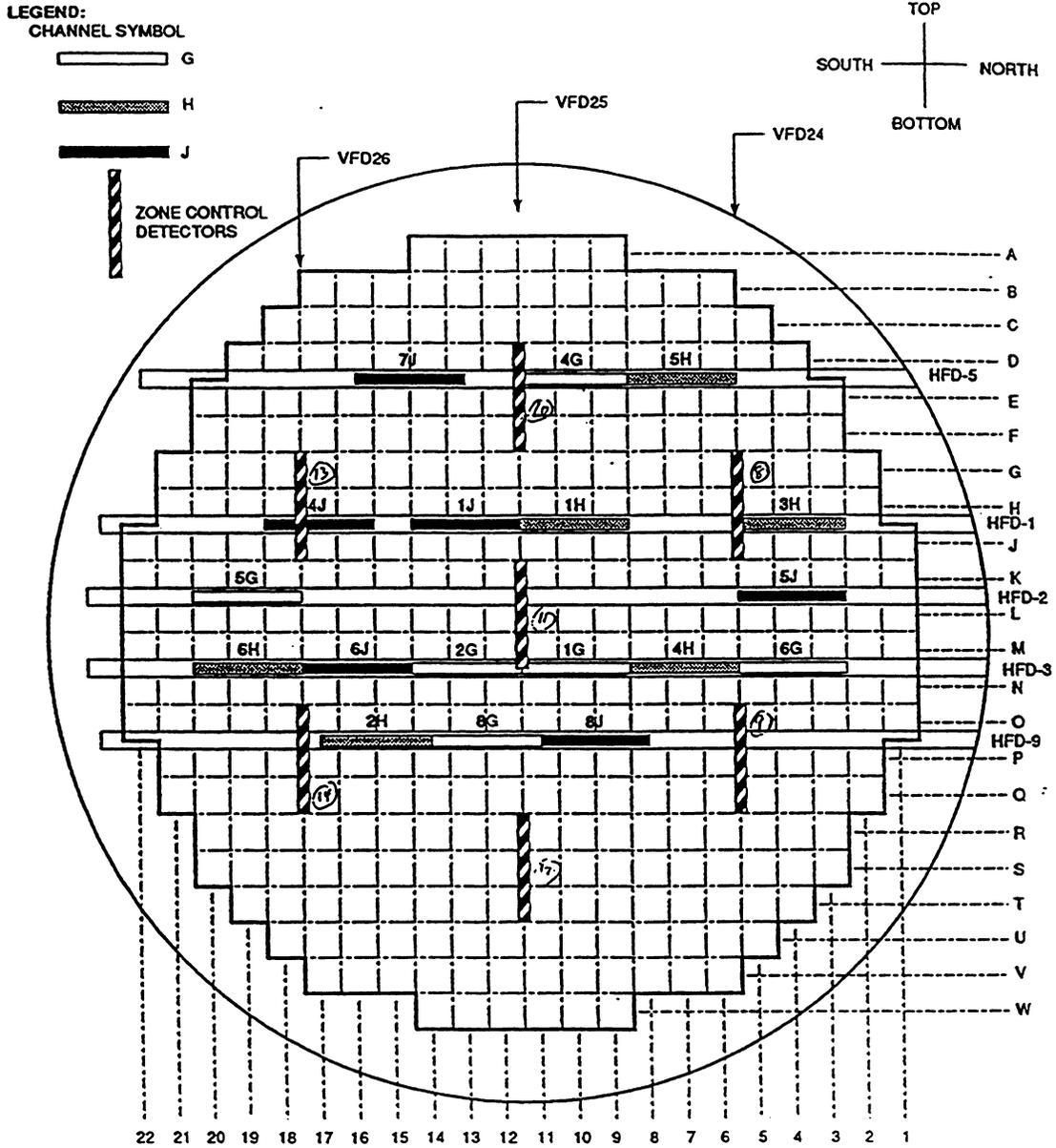
Figure 3: Detector Layouts

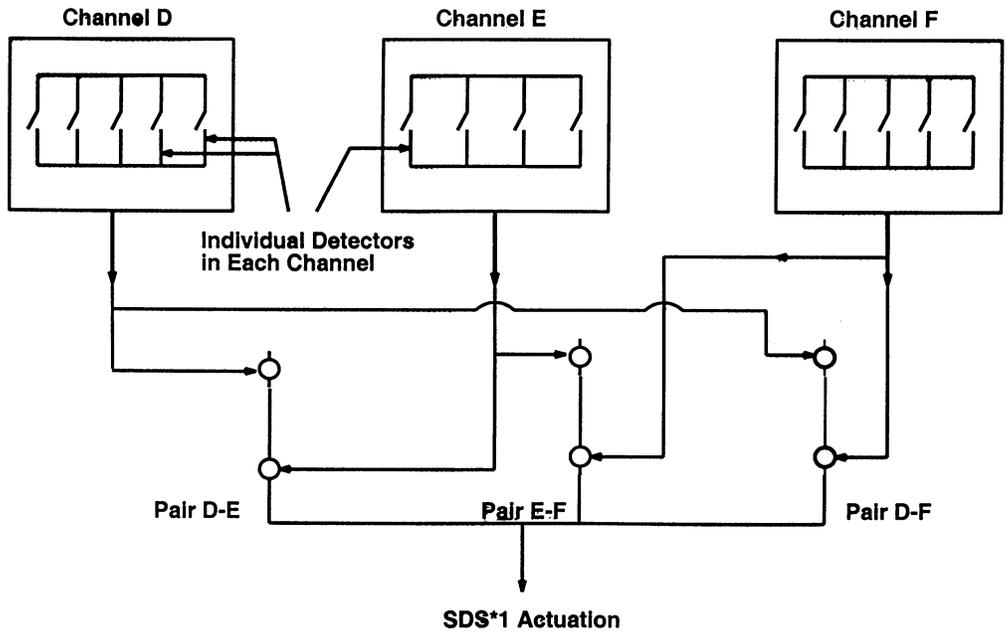Figure 4: Location of Horizontal In-Core ROP Detectors in a CANDU Reactor

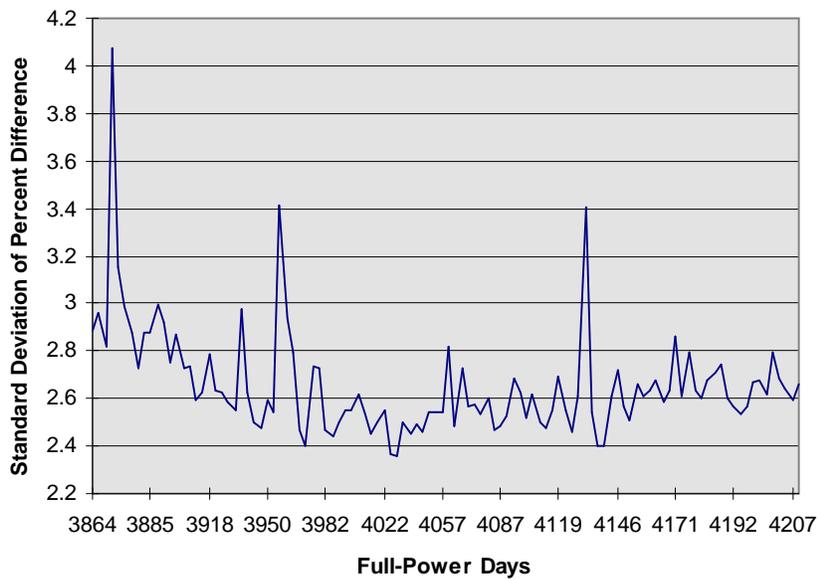Figure 5: Triplicated Logic for Shutdown System Number 1



Figure 6: Standard Deviation of Percent Difference Between Calculated and Measured Thermal Flux Values at In-Core Vanadium Detectors